

RESEARCH ARTICLE

Staphylococcus aureus single-stranded DNA-binding protein SsbA can bind but cannot stimulate PriA helicase

Yen-Hua Huang¹, Hong-Hsiang Guan², Chun-Jung Chen^{2,3,4*}, Cheng-Yang Huang^{1,5*}

1 School of Biomedical Sciences, Chung Shan Medical University, Taichung City, Taiwan, **2** Life Science Group, Scientific Research Division, National Synchrotron Radiation Research Center, Hsinchu, Taiwan, **3** Institute of Biotechnology, and University Center for Bioscience and Biotechnology, National Cheng Kung University, Tainan City, Taiwan, **4** Department of Physics, National Tsing Hua University, Hsinchu, Taiwan, **5** Department of Medical Research, Chung Shan Medical University Hospital, Taichung City, Taiwan

* cjchen@nsrrc.org.tw (CJC); cyluang@csmu.edu.tw (CYH)



Abstract

Single-stranded DNA-binding protein (SSB) and PriA helicase play important roles in bacterial DNA replication restart process. The mechanism by which PriA helicase is bound and stimulated by SSB in *Escherichia coli* (Ec) has been established, but information on this process in Gram-positive bacteria are limited. We characterized the properties of SSB from *Staphylococcus aureus* (SaSsbA, a counterpart of EcSSB) and analyzed its interaction with SaPriA. The gel filtration chromatography analysis of purified SaSsbA showed a stable tetramer in solution. The crystal structure of SaSsbA determined at 1.82 Å resolution (PDB entry 5XGT) reveals that the classic oligonucleotide/oligosaccharide-binding folds are formed in the N-terminal DNA-binding domain, but the entire C-terminal domain is disordered. Unlike EcSSB, which can stimulate EcPriA via a physical interaction between EcPriA and the C-terminus of EcSSB (SSB-Ct), SaSsbA does not affect the activity of SaPriA. We also found that SaPriA can be bound by SaSsbA, but not by SaSsbA-Ct. Although no effect was found with SaSsbA, SaPriA can be significantly stimulated by the Gram-negative *Klebsiella pneumoniae* SSB (KpSSB). In addition, we found that the conserved SSB-Ct binding site of KpPriA (Trp82, Tyr86, Lys370, Arg697, and Gln701) is not present in SaPriA. Arg697 in KpPriA is known to play a critical role in altering the SSB₃₅/SSB₆₅ distribution, but this corresponding residue in SaPriA is Glu767 instead, which has an opposite charge to Arg. SaPriA E767R mutant was constructed and analyzed; however, it still cannot be stimulated by SaSsbA. Finally, we found that the conserved MDFDDIPF motif in the Gram-negative bacterial SSB is DISDDDLPF in SaSsbA, i.e., F172 in EcSSB and F168 in KpSSB is S161 in SaSsbA, not F. When acting with SaSsbA S161F mutant, the activity of SaPriA was dramatically enhanced elevenfold. Overall, the conserved binding sites, both in EcPriA and EcSSB, are not present in SaPriA and SaSsbA, thereby no stimulation occurs. Our observations through structure-sequence comparison and mutational analyses indicate that the case of EcPriA-EcSSB is not applicable to SaPriA-SaSsbA because of inherent differences among the species.

OPEN ACCESS

Citation: Huang Y-H, Guan H-H, Chen C-J, Huang C-Y (2017) *Staphylococcus aureus* single-stranded DNA-binding protein SsbA can bind but cannot stimulate PriA helicase. PLoS ONE 12(7): e0182060. <https://doi.org/10.1371/journal.pone.0182060>

Editor: Giovanni Maga, Istituto di Genetica Molecolare, ITALY

Received: May 5, 2017

Accepted: July 11, 2017

Published: July 27, 2017

Copyright: © 2017 Huang et al. This is an open access article distributed under the terms of the [Creative Commons Attribution License](https://creativecommons.org/licenses/by/4.0/), which permits unrestricted use, distribution, and reproduction in any medium, provided the original author and source are credited.

Data Availability Statement: All relevant data are within the paper. Atomic coordinates and related structure factors have been deposited in the PDB with accession code 5XGT.

Funding: This research was supported by a grant from the Ministry of Science and Technology, Taiwan (MOST 105-2320-B-040-026 to C.Y. Huang). The funders had no role in study design, data collection and analysis, decision to publish, or preparation of the manuscript.

Competing interests: The authors have declared that no competing interests exist.

Introduction

Single-stranded DNA (ssDNA)-binding protein (SSB) is essential for DNA metabolic processes [1, 2]. The binding of SSB to ssDNA is independent of the sequence of DNA. SSB protects susceptible ssDNA from nucleolytic digestion and prevents the secondary structure formation of ssDNA [3]. In addition, SSB also binds to many DNA-binding proteins that constitute the SSB interactome [2, 4, 5]. The functions of SSB are well studied in *Escherichia coli* (EcSSB), and relatively little is known about SSB from other bacteria. SSBs are typically homotetramers [3, 6, 7], in which four oligonucleotide/oligosaccharide-binding folds (OB folds) form a DNA-binding domain [8–12]. However, SSB from the bacterial phylum *Deinococcus-Thermus* functions as a homodimer, in which each monomer contains two OB folds linked by a conserved spacer sequence [13–20]. SSB from *Sulfolobus solfataricus* is a monomer (one OB fold) [21–25]. Recently, a distinct SSB ThermoDBP is found to bind ssDNA without the classical OB folds of bacterial SSB [26, 27].

Bacterial SSBs consist of a conserved N-terminal ssDNA-binding/oligomerization domain (SSBn) and a flexible, highly disordered C-terminal protein–protein interaction domain (SSBc) [2, 28]. SSBc can be further subdivided into two sub-domains: a long proline- or glycine-rich hinge, also known as the intrinsically disordered linker (IDL) and, the highly conserved acidic tail of the last six C-terminal amino acid residues of SSB (DDDIPF) [2, 29]. This acidic tail of SSB binds to many DNA-binding proteins, and the activities of some of these proteins are stimulated by their interactions with ssDNA-bound SSB [2]. The binding of SSB to ssDNA makes IDL easily accessible to other proteins, such as proteases and DNA polymerase III [30, 31]. The C-terminus in SSB can also interact with the OB fold and regulate the ssDNA-binding activity of SSB itself [32, 33]. EcSSB has two major ssDNA binding modes [34]. In the (SSB)₃₅-binding mode, two subunits of the tetramer participate in ssDNA binding, whereas in the (SSB)₆₅-binding mode, all four subunits interact with ssDNA. The binding mode is dependent on the concentrations of protein and salt in the solution. During the different stages of DNA metabolism, different binding modes of SSB to ssDNA may be required for the in vivo function [35–37].

PriA is a DEXH-type helicase, utilized during replication restart to reload DnaB back onto the chromosome [38, 39]. Fuelled by the binding and hydrolysis of ATP, PriA moves along the nucleic acid filaments with other primosomal proteins and separates double-stranded DNA into their complementary single strands [40–42]. In *E. coli*, the replication restart primosome consists of PriA, PriB, PriC, DnaB helicase, DnaC, DnaT, and DnaG primase [38, 39, 43]. PriA recognizes stalled DNA replication forks with either duplex or SSB-coated ssDNA lagging strands and then processes for full primosome assembly [43–45]. However, PriA is a poor helicase when acting alone and might need other accessory proteins, such as PriB and SSB, to stimulate the helicase activity [46, 47]. The reaction mechanisms of DNA replication restart primosome are well studied in Gram-negative *E. coli* [43, 44, 48–53]. Relatively little is known about the regulation of the Gram-positive bacterial PriA-directed primosome activity [54, 55]. In the Gram-positive *Bacillus subtilis*, the initiator protein PriA helicase has a homolog of *E. coli* [56]. Nevertheless, PriB, PriC, DnaT, and DnaC proteins are not found in Gram-positive bacteria. Instead, Gram-positive *B. subtilis* has different primosomal proteins, namely, DnaD, DnaB, and DnaI, which are essential for replication restart [57]. Whether SSB functions and participates in the Gram-positive bacterial PriA-directed primosome assembly in a manner different from that of *E. coli* is still unknown.

In this study, we have cloned, expressed, purified, and crystallized the Gram-positive *Staphylococcus aureus* main SSB (SaSsbA) and determined its structure at 1.82 Å resolution. Basing on the results from surface plasmon resonance (SPR) experiments, ATPase stimulation effects

and structure-sequence analysis on SaSsbA–SaPriA interaction, we found that SaSsbA can bind but cannot stimulate SaPriA. Through domain deletion and structure-based mutational analyses, we conclude that the conserved binding sites, both in EcPriA and EcSSB, are not present in SaPriA and SaSsbA, thereby no stimulation occurs.

Materials and methods

Construction of plasmids for SaSsbA, tag-free SaSsbA, KpSSB, tag-free KpSSB, KpSSBc, SaDnaD, and SaPriA expression

Construction of the SaDnaD [58], SaPriA [59], *Klebsiella pneumoniae* SSB (KpSSB) [60], and tag-free KpSSB [61] expression plasmids has been reported. The gene encoding SaSsbA (the accession number ACY10277) was amplified by PCR using the genomic DNA of *S. aureus* subsp. *aureus* ED98 as template. The forward and reverse primers were designed to introduce unique restriction sites into SaSsbA, permitting the insertion of the amplified gene into the pET21b vector (Novagen Inc., Madison, WI, USA) for protein expression in *E. coli*. To obtain His tag-free SaSsbA, a fragment containing the coding sequence of SaSsbA and the stop codon was directly amplified and ligated into the pET21b vector. KpSSBc (aa 116–174) was also subcloned in the pET21b vector. Primers used for construction of these plasmids are summarized in Table 1.

Protein concentration

The protein concentration of the solutions was determined by the Bio-Rad Protein Assay using bovine serum albumin as a standard (Bio-Rad, CA, USA). The Bio-Rad Protein Assay is a dye-binding assay in which a differential color change of a dye occurs in response to various concentrations of protein [62].

Protein expression and purification

Purification of the recombinant SaDnaD [58], SaPriA [59], KpSSB [60], and tag-free KpSSB [61] has been reported. The recombinant SaSsbA and KpSSBc were expressed and purified

Table 1. Primers used for construction of plasmids.

Oligonucleotide	Primer
SaSsbA-NdeI-N	GGGCATATGCTAAATAGAGTTGTATTA
SaSsbA-XhoI-C	CCATTCTCGAGGAATGGTAAGTCATCA
Tag-free SaSsbA-NdeI-N	GGGCATATGCTAAATAGAGTTGTATTA
Tag-free SaSsbA-XhoI-C	CCATTCTCGAGTTAGAATGGTAAGTCATCA
KpSSBc-NdeI-N	GGGCATATGCGTCAGGGCGGCGCACCCG
KpSSBc-XhoI-C	GGGCTCGAGGAACGGGATGTCGTCGTCGAA
SaPriA E767R-N	TATAAAAGTGAACGTTGGATTATTACAAGCC
SaPriA E767R-C	TTGTAATAATCCACGTTCACTTTTATATTT
SaPriA R434A-N	GAAAGTTATGCAGCAGCTGAAAAGACGTT
SaPriA R434A-C	GTCTTTTTCAGCTGCTGCATAACTTTCAAG
SaSsbA S161F-N	GGACCGATTGATATATTCGATGATGACTTACCA
SaSsbA S161F-C	GTCATCATCGAATATATCAATCGGTCCGTTTGC
SaSsbA S161F/dell160-N	GGACCGATTGATTTTCGATGATGACTTACCA
SaSsbA S161F/dell160-C	TAAGTCATCATCGAAATCAATCGGTCCGTT

These plasmids were verified by DNA sequencing. Underlined nucleotides indicate the designated site for the restriction site or the mutation site.

<https://doi.org/10.1371/journal.pone.0182060.t001>

using the protocol described previously for PriB [63]. Briefly, *E. coli* BL21(DE3) cells were transformed with the expression vector and overexpression of the expression plasmids was induced by incubating with 1 mM isopropyl thiogalactopyranoside. The protein was purified from the soluble supernatant by Ni²⁺-affinity chromatography (HiTrap HP; GE Healthcare Bio-Sciences), eluted with Buffer A (20 mM Tris-HCl, 250 mM imidazole, and 0.5 M NaCl, pH 7.9), and dialyzed against a dialysis buffer (20 mM HEPES and 100 mM NaCl, pH 7.0; Buffer B). Protein purity remained at >97% as determined by SDS-PAGE (Mini-PROTEAN Tetra System; Bio-Rad, CA, USA).

The recombinant tag-free SaSsbA was expressed and purified using the protocol described previously [61] for *Pseudomonas aeruginosa* SSB (PaSSB) and *Salmonella enterica* serovar Typhimurium LT2 SSB (StSSB) with the following modifications. The cells overexpressing the protein were chilled on ice, harvested by centrifugation, resuspended in Buffer C (20 mM Tris-HCl and 50 mM NaCl, pH 7.9) and disrupted by sonication with ice cooling. The protein solution (50 mL) was precipitated from the supernatant of the cell lysate by incubation with 0.27 g/mL of ammonium sulfate for 30 min and centrifugation at 20000g for 10 min. The pellets were washed twice with 2.0 mL of Buffer D (20 mM Tris-HCl, 50 mM NaCl, and 1.2 M ammonium sulfate, pH 7.9). After dialysis against Buffer C, the protein solution applied to the Q column (GE Healthcare Bio-Sciences, Piscataway, NJ, USA) was eluted with a linear NaCl gradient from 0.1 to 0.6 M with Buffer C using the AKTA-FPLC system (GE Healthcare Bio-Sciences, Piscataway, NJ, USA). The peak fractions with the ssDNA binding activity were collected and dialyzed against Buffer E (20 mM potassium phosphate, 1 mM EDTA, and 100 mM NaCl, pH 7.0). The protein solution was then applied to the Heparin HP column (GE Healthcare Bio-Sciences, Piscataway, NJ, USA) and eluted with a linear NaCl gradient from 0.1 to 1.0 M with Buffer E. The peak fractions from this chromatographic step with the ssDNA binding activity were collected and concentrated, and the purity of tag-free SaSsbA remained at >97% as determined by SDS-PAGE.

Gel-filtration chromatography

Gel-filtration chromatography was carried out by the AKTA-FPLC system (GE Healthcare Bio-Sciences, Piscataway, NJ, USA). In brief, purified SaSsbA (2 mg/mL) in Buffer B was applied to a Superdex 200 prep grade column (GE Healthcare Bio-Sciences, Piscataway, NJ, USA) equilibrated with the same buffer. The column was operated at a flow rate of 0.5 ml/min, and 0.5-ml fractions were collected. The proteins were detected by measuring the absorbance at 280 nm. The column was calibrated with proteins of known molecular weight: thyroglobulin (670 kDa), γ -globulin (158 kDa), albumin (67 kDa), ovalbumin (43 kDa), chymotrypsinogen A (25 kDa) and ribonuclease A (13.7 kDa). The K_{av} values for the standard proteins and SaSsbA were calculated from the equation: $K_{av} = (V_e - V_o)/(V_c - V_o)$, where V_o is column void volume, V_e is elution volume, and V_c is geometric column volume.

Electrophoretic mobility shift assay (EMSA)

EMSA for SaSsbA was conducted using the protocol described previously for SSB [64]. Briefly, radiolabeling of various lengths of ssDNA oligonucleotides was carried out with [γ ³²P]ATP (6000 Ci/mmol; PerkinElmer Life Sciences, Waltham, MA) and T4 polynucleotide kinase (Promega, Madison, WI, USA). The protein (0, 0.037, 0.075, 0.15, 0.31, 0.62, 1.25, 2.5, 5, and 10 μ M; monomer) was incubated for 30 min at 25°C with 1.7 nM DNA substrates in a total volume of 10 μ L in 20 mM Tris-HCl pH 8.0 and 100 mM NaCl. Aliquots (5 μ L) were removed from each of the reaction solutions, and added to 2 μ L of gel-loading solution (0.25% bromophenol blue and 40% sucrose). The resulting samples were resolved on a native 8% polyacrylamide gel at

4°C in TBE buffer (89 mM Tris borate and 1 mM EDTA) for 1 h at 100 V, and were visualized by phosphorimaging. The phosphor storage plate was scanned, and the data for complex and free DNA bands were digitized for quantitative analysis. The ssDNA binding ability for the protein was estimated using linear interpolation from the protein concentration that binds 50% of the input DNA. Each $[\text{Protein}]_{50}$ was calculated as the average of at least three measurements \pm S.D.

Preparation of dsDNA substrate

The double-stranded DNA substrates (dsDNA) were prepared with a radiolabeled PS4 strand (3' -GGGCTTAAGCCTATCGAGCCATGGG-5'; 25 mer) and an unlabeled PS3-dT30 strand (5' -CCCGAATTCCGATAGCTCGGTACCC-dT30-3') at a 1:1 concentration ratio. Each dsDNA substrate was formed in 20 mM HEPES (pH 7.0) and 100 mM NaCl, by brief heating at 95°C for 5 min and then followed by slow cooling to room temperature overnight.

Surface plasmon resonance (SPR)

SPR was conducted using the protocol described previously for DnaC helicase [65]. SaPriA was immobilized on Series S sensor chips CM5 (GE Healthcare Bio-Sciences, Piscataway, NJ, USA). The SaPriA-binding experiments were carried out at 293K using a Biacore T200 (GE Healthcare Bio-Sciences, Piscataway, NJ, USA) with running buffer (40 mM Tris, 200 mM NaCl, and 0.05% Tween-20 at pH 8.0). SaSsbA solutions were diluted in the running buffer to final concentrations of 1000, 500, 250, 125, and 63 nM. The Diluted samples were injected in duplicate over the immobilized protein for 120 s at a flow rate of 30 $\mu\text{L}/\text{min}$. The running buffer was then flushed for 300 s at a flow rate of 30 $\mu\text{L}/\text{min}$. Finally, the chip surface was regenerated by injecting 2 M MgCl_2 buffer for 60 s at a flow rate of 30 $\mu\text{L}/\text{min}$. Control samples were used to monitor the sensor chip surface stability, demonstrating reproducibility throughout the duration of the experiments. The estimated K_d values were derived by fitting the association and dissociation signals with a 1:1 (Langmuir) model using the Biacore T200 Evaluation Software. Chemically synthesized peptides SaSsbA-Ct (NANGPIDISDDDLPF) and KpSSB-Ct (PSNEPPMDFDDDI PF) were also used (4–7 different concentrations ranging from 0.06 to 2 μM) for SaPriA-binding experiments.

ATPase assay

SaPriA ATPase assay [58] was performed with 0.4 mM $[\gamma\text{-}^{32}\text{P}]$ ATP and 0.12 μM of SaPriA in reaction buffer containing 40 mM Tris (pH 8.0), 10 mM NaCl, 2 mM DTT, 2.5 mM MgCl_2 , and 0.1 μM PS4/PS3-dT30 DNA substrate. Aliquots (5 μL) were taken and spotted onto a polyethyleneimine cellulose thin-layer chromatography plate, which was subsequently developed in 0.5 M formic acid and 0.25 M LiCl for 30 m. Reaction products were visualized by autoradiography and quantified with a phosphorimager.

Crystallography

Before crystallization, SaSsbA was concentrated to 20 mg/mL in Buffer B. Crystals were grown at room temperature by hanging drop vapor diffusion in 22% PEG 4000, 100 mM HEPES, 100 mM sodium acetate, pH 7.5. Data were collected using an ADSC Quantum-315r CCD area detector at SPXF beamline BL13C1 at NSRRC (Taiwan, ROC). All data integration and scaling were carried out using HKL-2000 [66]. There were two SaSsbA monomers per asymmetric unit. The crystal structure of SaSsbA was solved at 1.82 Å resolution with the molecular replacement software AMoRe [67] using *Mycobacterium smegmatis* SSB as model (PDB entry 1X3E).

After molecular replacement, model building was carried out using XtalView [68]. CNS was used for molecular dynamic refinement [69]. The final structure was refined to an R -factor of 0.1932 and an R_{free} of 0.2233. Atomic coordinates and related structure factors have been deposited in the PDB with accession code 5XGT.

Bioinformatics

The amino acid sequences of 417 sequenced PriA and 484 SSB homologs were aligned using ConSurf [70]. The model of SaPriA was built from the coordinates of 4NL4 (crystal structure of KpPriA) by using SWISS-MODEL, <http://swissmodel.expasy.org/>. The structures were visualized by using the program PyMol.

Results

Analysis of the *ssb* (SAAV_0334) gene

Based on the similar nucleotide sequence to *E. coli* SSB, the gene SAAV_0334, which encodes *S. aureus* main SSB, was initially found using a database search through the National Center for Biotechnology Information (NCBI). In this study, this SSB was designated as SsbA. Fig 1 shows the map of *S. aureus*, in which the *ssb* gene is flanked by the *rpsF* and *rpsR* genes, coding for the ribosomal proteins S6 and S18, respectively. Unlike *E. coli* *ssb* gene organization, *S. aureus* and *B. subtilis* *ssb* genes are not located adjacent to *uvrA* gene. These genes (*rpsF*, *ssb*, and *rpsR*) in *B. subtilis* belong to one operon and are controlled by the SOS response [71].

Sequence analysis of SaSsbA

The gene SAAV_0334, which encodes *S. aureus* SsbA (SaSsbA), was initially found using a database search through NCBI. Based on the known nucleotide sequence, the predicted SaSsbA monomer protein has a length of 167 amino acid residues and a molecular mass of 19 kDa. Analysis of the sequence of SaSsbA by RPS-BLAST showed the presence of a putative OB-fold domain that is common in all known SSBs. Fig 2 shows the alignment consensus of 484 sequenced SSB homologs by ConSurf [70], revealing the degree of variability at each position along the sequence. In the EcSSB–ssDNA complex [72], four essential aromatic residues, Trp40, Trp54, Phe60, and Trp88, conserved in most SSB families as Phe/Tyr/Trp, participate in ssDNA binding via stacking interactions. The corresponding residues in SaSsbA are Phe37, Phe48, Phe54, and Tyr82; no Trp residue was observed in SaSsbA. The important C-terminal tail DDDIPF of EcSSB involved in protein–protein interaction is DDDLPF in SaSsbA.

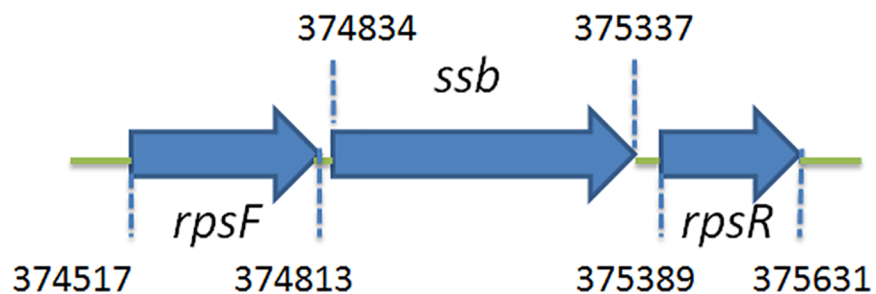


Fig 1. Gene map of *S. aureus* chromosomal region with *ssb*. The gene SAAV_0334 coding for SSB (designated as SsbA in this study) maps from the 374834 to 375337 nt of the *S. aureus* genome. This *ssb* gene is flanked by the *rpsF* and *rpsR* genes, coding for the ribosomal proteins S6 and S18, respectively.

<https://doi.org/10.1371/journal.pone.0182060.g001>



Fig 2. Sequence analysis of SaSsbA. An alignment consensus of 484 sequenced SSB homologs by ConSurf reveals the degree of variability at each position along the sequence. Highly variable amino acid residues are colored teal, whereas highly conserved amino acid residues are burgundy. A consensus sequence was established by determining the most commonly found amino acid residue at each position relative to the sequence of SaSsbA.

<https://doi.org/10.1371/journal.pone.0182060.g002>

Sequence analysis of SaPriA

Based on the known nucleotide sequence, the predicted SaPriA monomer protein has a length of 802 amino acid residues (which is higher than that for EcPriA with 732 amino acid residues) and a molecular mass of 92.7 kDa, with a pI of 6.12. Analysis of the structure of SaPriA indicated a DEAD-like helicase (aa 288–427) and revealed the presence of the putative Mg²⁺ ion binding site (aa 388–391), ATP-binding sites (aa 295–299, 618, 651, 655, and 658), and nucleotide-binding region (580, 581, and 610–612). Fig 3 shows that the alignment consensus of 417 sequenced PriA homologs by ConSurf revealed the degree of variability at each position along the sequence, in which the binding sites mentioned above are highly conserved among varying organisms. Amino acid residues in the C-terminal helicase domain of PriA are also conserved. However, amino acid residues in the N-terminal region of SaPriA, especially aa 114–286, are variable. Given that distinct mechanisms exist for reloading the replicative DnaB helicase by the Gram-positive and Gram-negative bacterial PriA, whether or not this highly variable region (aa 114–286) in SaPriA is responsible for binding by the Gram-positive bacterial specific helicase loader is still unknown.

Purification of SaSsbA and tag-free SaSsbA

The gene *SAAV_0334* encoding for the putative SaSsbA was PCR-amplified using the genomic DNA of *S. aureus* subsp. *aureus* ED98 as template. This amplified gene was then ligated into the pET21b vector for protein expression. SaSsbA with a Hig tag was heterologously overexpressed in *E. coli* and then purified from the soluble supernatant by Ni²⁺-affinity chromatography. Pure protein was obtained in this single chromatographic step with an elution of Buffer A and dialyzed against a dialysis buffer (Buffer B). Approximately >10 mg of purified protein was obtained from 1 L of *E. coli* cell culture. To exclude the possible effect of a His tag, tag-free SaSsbA was also produced and purified by precipitation of ammonia sulfate, Q, and Heparin column chromatographies. Approximately 2 mg of purified tag-free SaSsbA was obtained from 1 L of *E. coli* cell culture.

SaSsbA bound to ssDNA

To investigate the length of nucleotides needed for the formation of the SaSsbA–ssDNA complex, as well as the ssDNA-binding ability of SaSsbA, we studied the binding of SaSsbA to dT15, dT20, dT30, and dT40 with different protein concentrations (Fig 4). The binding ability of SaSsbA to dT40 in the presence of 0.4 M NaCl was also analyzed (Fig 4). As shown in Fig 4A, no significant band shift was observed when SaSsbA was incubated with dT15, indicating

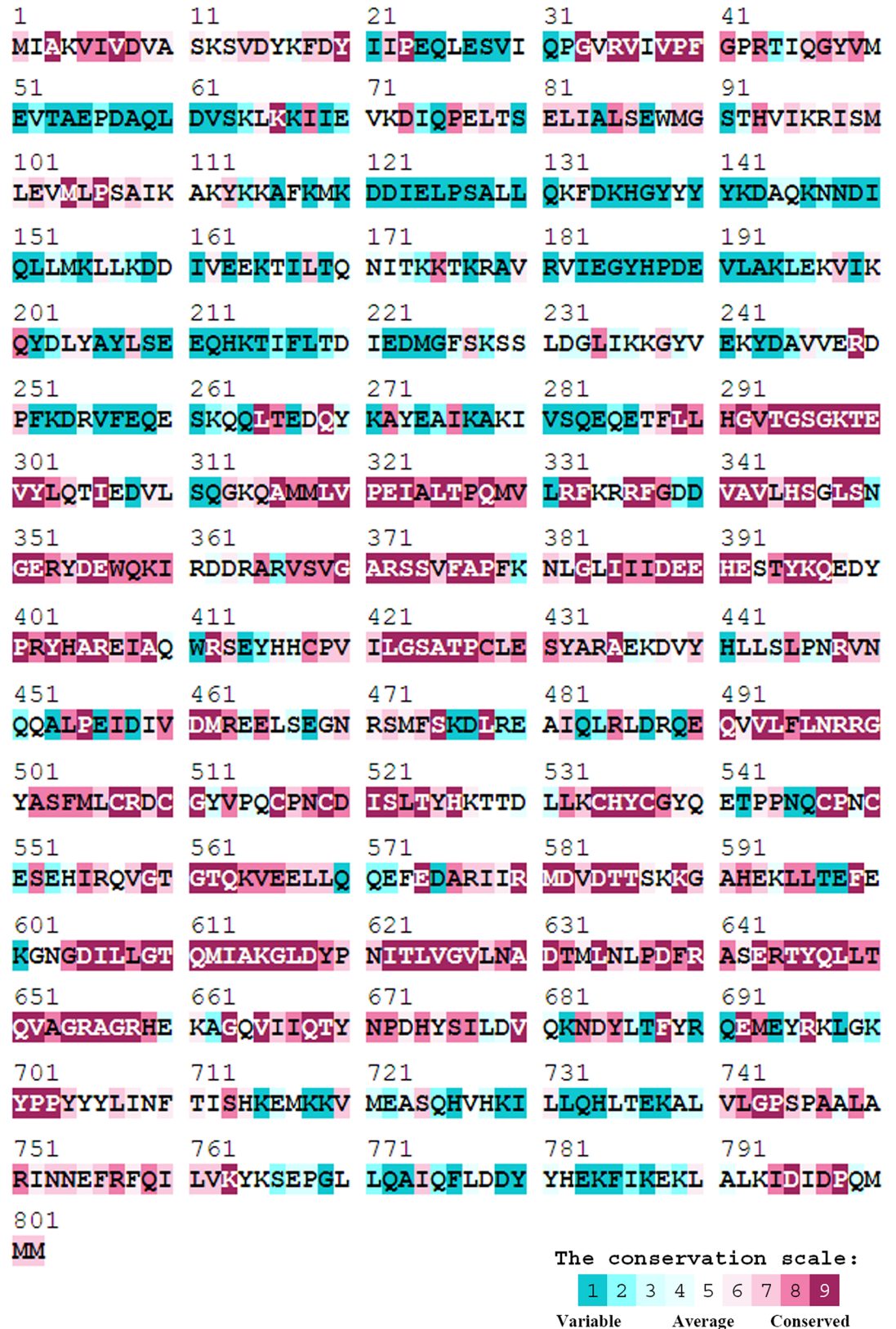


Fig 3. Sequence analysis of SaPriA. An alignment consensus of 417 sequenced PriA homologs by ConSurf reveals the degree of variability at each position along the sequence. In general, amino acid residues in the C-terminal region of PriA are conserved.

<https://doi.org/10.1371/journal.pone.0182060.g003>

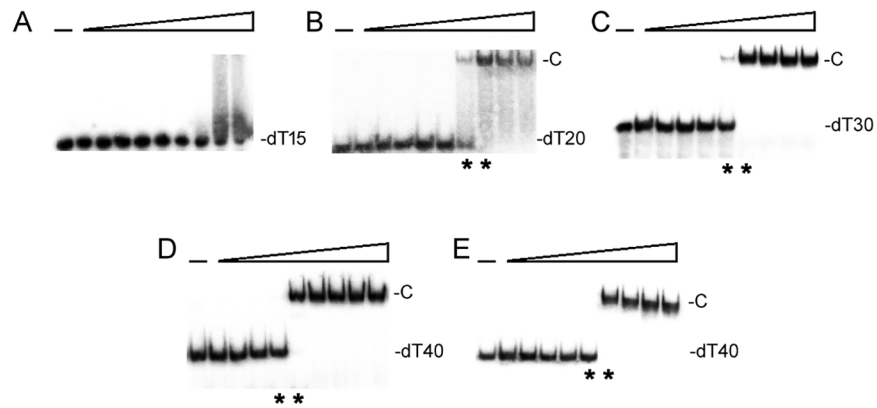


Fig 4. EMSA of SaSsbA. Protein (0, 0.037, 0.075, 0.15, 0.31, 0.62, 1.25, 2.5, 5, and 10 μ M; monomer) was incubated at 25°C for 30 min with 1.7 nM of (A) dT15, (B) dT20, (C) dT30, or (D) dT40 in a total volume of 10 μ L in 20 mM Tris-HCl (pH 8.0) and 100 mM NaCl. (E) The binding of SaSsbA to dT40 in the presence of 0.4 M NaCl. The $[\text{Protein}]_{50}$ values of SaSsbA as a function of the length of the ssDNA were determined using EMSA. Protein concentrations used to determine the midpoint values are indicated by asterisks.

<https://doi.org/10.1371/journal.pone.0182060.g004>

that SaSsbA could not form a stable complex with this homopolymer. By contrast to dT15, longer dT homopolymers, which include dT20–40, produced a significant band shift (C, complex), i.e., formation of a stable protein–DNA complex in solution. To compare the binding abilities of SaSsbA with ssDNA of different lengths, the midpoint values for input ssDNA binding that were calculated from the titration curves of EMSA and the $[\text{Protein}]_{50}$ values were quantified using linear interpolation from the protein concentration and are summarized in Table 2. The $[\text{SaSsbA}]_{50}$ for dT40 binding is 90 ± 5 nM, which is twofold lower than that in the presence of 0.4 M NaCl (180 ± 22 nM).

Oligomeric state of SaSsbA in solution

The oligomeric state of purified SaSsbA was analyzed by gel filtration chromatography (Fig 5), and the native molecular mass of SaSsbA was estimated to be 77 kDa. The native molecular mass for SaSsbA is approximately 4 times the molecular mass of a SaSsbA monomer (19 kDa). Thus, we concluded that SaSsbA in solution is a stable tetramer like EcSSB.

SaSsbA cannot stimulate the ATPase activity of SaPriA

PriA is known as a poor helicase when acting alone in vitro [72]. Gram-negative EcPriA activity can be significantly stimulated by PriB and SSB [46, 47]. Recently, we also found that

Table 2. The $[\text{Protein}]_{50}$ values of SaSsbA as analyzed by EMSA.

DNA	$[\text{Protein}]_{50}$ (nM)
dT15	> 2000
dT20	292 ± 28
dT30	186 ± 20
dT40	90 ± 5
dT40 (with 0.4 M NaCl)	180 ± 22

$[\text{Protein}]_{50}$ was calculated from the titration curves of EMSA by determining the concentration of the protein needed to achieve the midpoint value for input DNA binding. Errors are standard deviations determined by three independent titration experiments.

<https://doi.org/10.1371/journal.pone.0182060.t002>

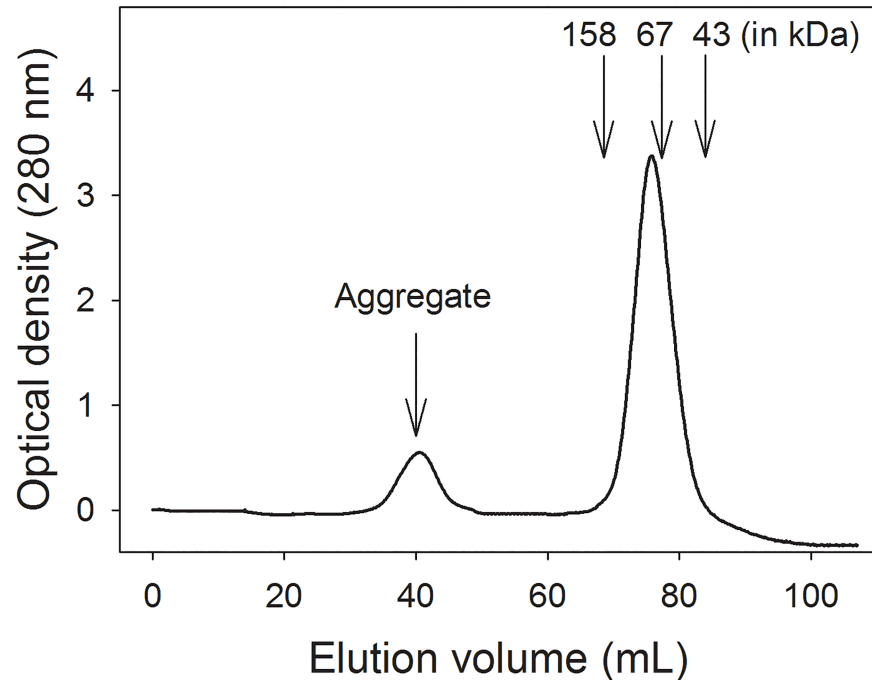


Fig 5. Oligomeric state of purified SaSsbA in solution. Purified protein in Buffer B was applied to a Superdex 200 prep grade column equilibrated with the same buffer. The column was calibrated with proteins of known molecular masses: thyroglobulin (670 kDa), γ -globulin (158 kDa), albumin (67 kDa), ovalbumin (43 kDa), chymotrypsinogen A (25 kDa) and ribonuclease A (13.7 kDa). The corresponding peak shows the eluted SaSsbA.

<https://doi.org/10.1371/journal.pone.0182060.g005>

SaDnaD can significantly enhance the activity of SaPriA [58]. Whether SaSsbA can stimulate SaPriA activity is unknown. SaPriA could hydrolyze ATP alone; however, no effect was found on the SaPriA activity when acting with SaSsbA (Fig 6). To exclude the possible effect of a His tag, tag-free SaSsbA was also used for this experiment, and a similar result was found. When tag-free SaSsbA was present at higher concentration (20 μ M), a similar result was still found (Fig 6). Thus, in contrast to the case in EcPriA, SaSsbA does not affect the activity of SaPriA.

Crystal structure of SaSsbA

To obtain an in-depth understanding of the structure–function relationship of SaSsbA and of the explanation why it cannot produce the same effect on SaPriA as EcSSB did on EcPriA, we crystallized SaSsbA and determined its structure at a resolution of 1.82 Å (Table 3). The secondary structural element of SaSsbA is shown in Fig 7A. The cell unit contains two monomers of SaSsbA (Fig 7B), but its oligomerization state in solution is tetrameric (Figs 5 and 7C). The SaSsbA monomer has an OB-fold domain similar to EcSSB, and the core of the OB-fold possesses a β -barrel capped by an α -helix. In both subunits, the majority of the electron density, only for the N-terminal region of SaSsbA, exhibited good quality (aa 1–104); the aa 105–167 was unobserved. In the EcSSB–ssDNA complex, four essential aromatic residues, Trp40, Trp54, Phe60, and Trp88, participate in ssDNA binding via stacking interactions. The corresponding residues in SaSsbA are Phe37, Phe48, Phe54, and Tyr82, may play a similar role in ssDNA binding as EcSSB (Fig 7D). Although the N-terminal domains of SaSsbA and EcSSB are similar, their loops L₁₂ and L₂₃ are structurally different, one is short, and the other is extended (Fig 7C). Structurally, SaSsbA also resembled PriB (Fig 7E), in which the only significant difference is in the lengths of the β 4 and β 5 sheets.

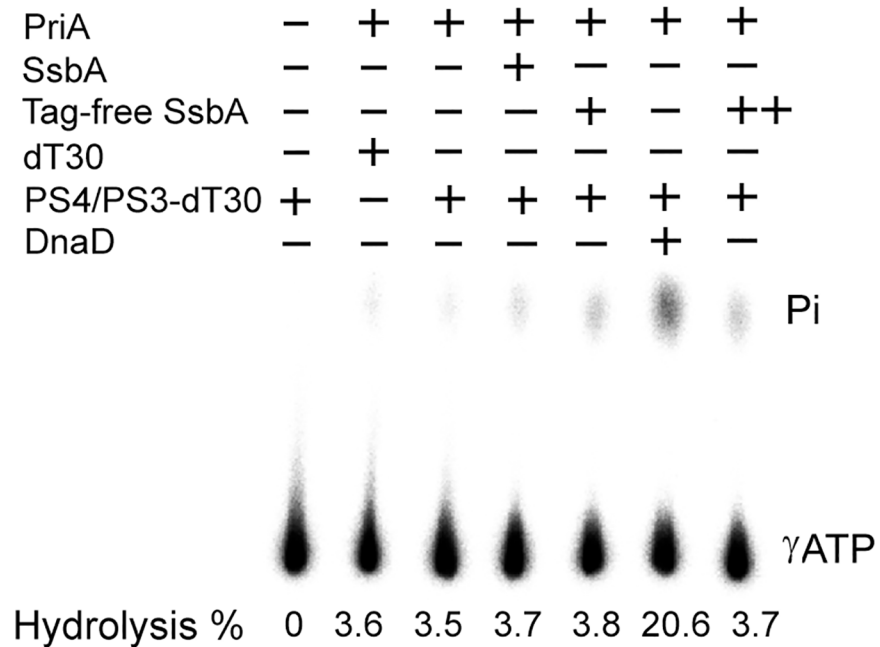


Fig 6. The ATPase activity of SaPriA did not change when acting with SaSsbA. SaPriA ATPase assay was performed with 0.4 mM [γ - 32 P] ATP, 0.12 μ M of SaPriA, and 0.1 μ M PS4/PS3-dT30 (or dT30) DNA substrate for 1 h. To study the effect, SaSsbA (10 μ M), tag-free SaSsbA (10 μ M), or SaDnaD (4 μ M) was added into the assay solution. Higher concentration of tag-free SaSsbA (20 μ M; denotes ++) was also used in this study. Aliquots (5 μ L) were taken and spotted onto a polyethyleneimine cellulose thin-layer chromatography plate, which was subsequently developed in 0.5 M formic acid and 0.25 M LiCl for 30 m. Reaction products were visualized by autoradiography and quantified with a Phosphorimager.

<https://doi.org/10.1371/journal.pone.0182060.g006>

Conserved SSB-Ct binding site of PriA is not present in SaPriA

PriA interacts with the SSB-Ct at replication forks [47, 73, 74]. In addition, this interaction is a driving force to stimulate the PriA activity [47]. The crystal structure of KpPriA in complex with an SSB-Ct peptide, which was determined at 4.1 Å resolution, reveals a specific and conserved binding pocket in PriA [44]. The KpPriA SSB-Ct binding site includes Trp82, Tyr86, Lys370, Arg697, and Gln701, in which Arg697 is located near the α -carboxyl group of the C-terminal-most residue of the SSB-Ct (Fig 8A) and plays a critical role in altering the SSB₃₅/SSB₆₅ distribution [44]. Interestingly, however, we found that such an important residue in EcPriA, namely, Arg697, is not conserved (Fig 2). The corresponding residue in SaPriA is Glu767 instead (Fig 8B and S1 Fig), which could possibly be the reason for the inability of SaSsbA to stimulate SaPriA. To have an Arg residue in the SSB-Ct binding site of SaPriA as KpPriA, we then constructed and analyzed the mutant SaPriA E767R, but still produced a similar result as the wild-type SaPriA did (Fig 8C). Furthermore, we found another Arg (Arg434) near the SSB-Ct pocket in SaPriA, which may play a similar role as the Arg697 in EcPriA; however, no difference was observed in the ATPase activity for the mutant SaPriA R434A (Fig 8C). Thus, whether the SSB-Ct binding site in SaPriA contains Arg or not is not crucial for SaPriA activation by SaSsbA.

SaPriA binds to SaSsbA, but not to the SSB-Ct peptide

EcPriA is known to bind SSB-Ct [47], and complexed crystal structure of KpPriA further showed this binding pocket [44]. In this study, we found that the binding site of KpPriA to

Table 3. Data collection and processing statistics.

Data collection			
	Crystal	SaSsbA	
	Wavelength (Å)	0.975	
	Resolution (Å)	30–1.76	
	Space group	P4 ₁ 2 ₁ 2	
	Cell dimension (Å)	a = 88.792	α = 90
		b = 88.792	β = 90
		c = 57.686	γ = 90
	Completeness (%)	99.8 (99.9)*	
	<I/σI>	34.6 (3.2)	
	R _{sym} or R _{merge} (%)	0.052 (0.559)	
	Redundancy	8.6 (8.4)	
Refinement			
	Resolution (Å)	28.078–1.82	
	No. reflections	23454	
	R _{work} /R _{free}	0.1932/0.2233	
	No. atoms		
	Protein	209	
	Water	110	
R.m.s deviation			
	Bond lengths (Å)	0.0179	
	Bond angles (°)	1.8595	
Ramachandran Plot			
	In preferred regions	192 (93.66%)	
	In allowed regions	8 (3.9%)	
	Outliers	5 (2.44%)	
	PDB entry	5XGT	

*Values in parentheses are for the highest resolution shell.

R_{sym} = Σ||I - <I>|/ΣI, where I is the observed intensity, <I> is the statistically weighted average intensity of multiple observations of symmetry-related reflections.

<https://doi.org/10.1371/journal.pone.0182060.t003>

SSB-Ct is not found in SaPriA (Fig 8), and SaSsbA failed to stimulate SaPriA (Fig 6). To confirm whether SaPriA interacts with SaSsbA, we used SPR to provide experimental evidence for estimating the binding affinity between these proteins and thus quantitatively characterize this interaction further (Fig 9). SaPriA was immobilized on a sensor chip (as a ligand), and the SaSsbA solution (as an analyte) was passed over the sensor chip in a microfluidic chamber. Fig 9A shows the SPR results at various SaSsbA concentrations. The K_d value of SaPriA bound by SaSsbA, calculated from the equilibrium binding isotherms using a simple binding model (a 1:1 Langmuir binding model), was 4.6 ± 0.5 × 10⁻⁸ M. Thus, even no identical binding site as in KpPriA, SaPriA can bind to SaSsbA.

To determine whether SaPriA can bind to SaSsbA-Ct (NANGPIDISSDDLPF) and KpSSB-Ct (PSNEPPMDFDDDI PF), chemically synthesized SaSsbA-Ct and KpSSB-Ct were used for SaPriA-binding experiments. SaSsbA-Ct was injected at increasing concentrations, but the binding response for SaPriA did not change, indicating no interaction (Fig 9B). No interaction of KpSSB-Ct with SaPriA was also found (Fig 9C). Therefore, unlike EcPriA, which binds to EcSSB-Ct directly, SaPriA cannot bind to SaSsbA-Ct and KpSSB-Ct.

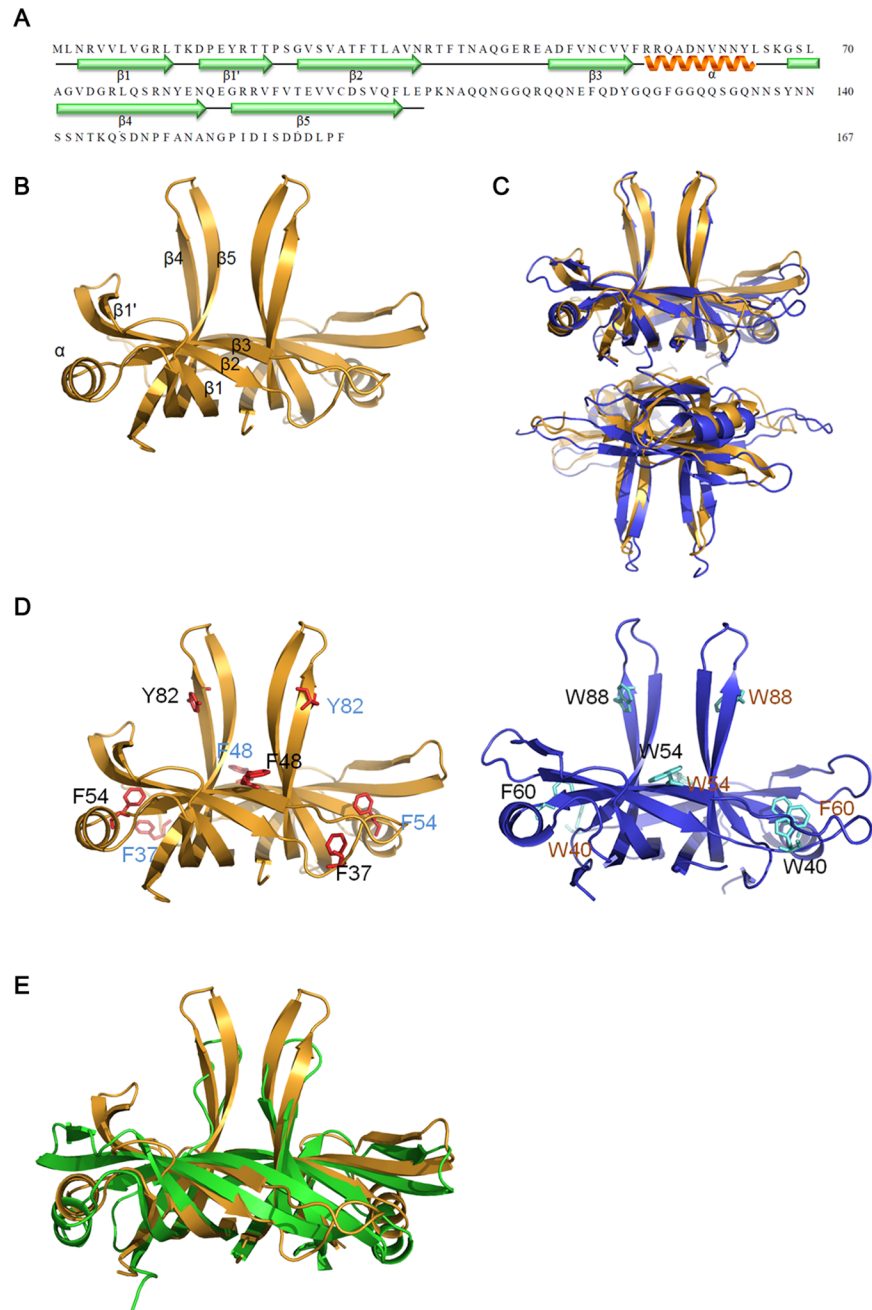


Fig 7. Crystal structure of SaSsbA. (A) The secondary structural element of SaSsbA. The secondary structural element of SaSsbA is shown above its sequence. (B) Crystal structure of SaSsbA. The cell unit contains two monomers of SaSsbA, and the core of the OB-fold possesses a β -barrel capped by an α -helix. In both subunits, the majority of the electron density exhibited good quality only for the N-terminal region of SaSsbA (aa 1–104); the aa 105–167 was unobserved. (C) Superposition of SaSsbA and EcSSB. The N-terminal domains of SaSsbA and EcSSB (PDB entry 1EYG; dark blue) are similar, but the structural differences are still found, the loops L₁₂ and L₂₃. Because the oligomerization state of SaSsbA in solution is tetrameric, SaSsbA may function as a tetramer like EcSSB. (D) ssDNA-binding mode of SaSsbA. In the EcSSB–ssDNA complex (PDB entry 1EYG), four essential aromatic residues, including Trp40, Trp54, Phe60, and Trp88, participate in ssDNA binding via stacking interactions. The structurally corresponding residues in SaSsbA are Phe37, Phe48, Phe54, and Tyr82. The ssDNA-binding mode of SaSsbA may be similar to that of EcSSB. (E) Superposition of SaSsbA and KpPriB. The N-terminal domain of SaSsbA and KpPriB (PDB entry 4APV; green) are similar, in which the only significant difference is in the lengths of the β 4 and β 5 sheets.

<https://doi.org/10.1371/journal.pone.0182060.g007>

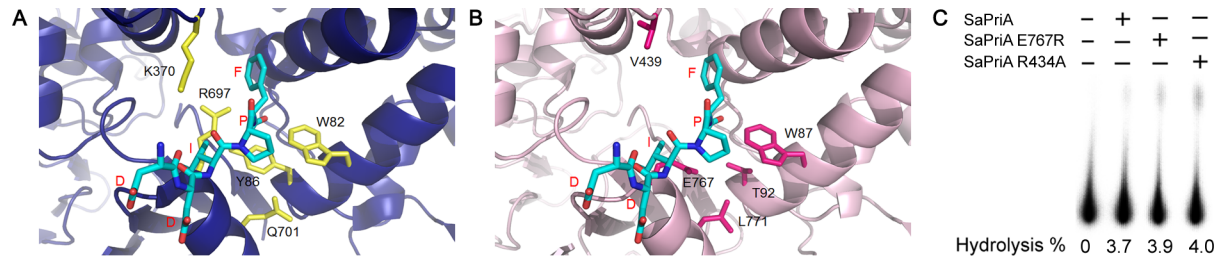


Fig 8. Conserved SSB-Ct binding site of PriA is not present in SaPriA. (A) SSB-Ct (DDIPF) binding site in KpPriA revealed by the complexed crystal structure (PDB ID: 4NL8). The KpPriA SSB-Ct binding site includes Trp82, Tyr86, Lys370, Arg697, and Gln701. (B) The putative SSB-Ct binding sites in SaPriA structurally corresponding with those in KpPriA are Trp89, Thr92, V439, Glu767, and Leu771. Only Trp89 in SaPriA (Trp82 in KpPriA) is conserved. Arg697, the most important residue in KpPriA in altering the SSB₃₅/SSB₆₅ distribution, is Glu767 in SaPriA. (C) Mutational analysis of SaPriA. The ATPase assay for the mutant SaPriA E767R and SaPriA R434A proteins was performed with 0.4 mM [γ -³²P] ATP, 0.12 μ M of the protein, SaSsbA (10 μ M), and 0.1 μ M PS4/PS3-dT30 DNA substrate for 1 h. Aliquots (5 μ L) were taken and spotted onto a polyethyleneimine cellulose thin-layer chromatography plate, which was subsequently developed in 0.5 M formic acid and 0.25 M LiCl for 30 m. Reaction products were visualized by autoradiography and quantified with a Phosphorimager.

<https://doi.org/10.1371/journal.pone.0182060.g008>

KpSSB, but not KpSSB-Ct, can significantly stimulate the ATPase activity of SaPriA

The typical SSB-Ct binding site of PriA in SaPriA is not conserved (Fig 8). To investigate whether all SSB cannot stimulate SaPriA like SaSsbA, the ATPase activity of SaPriA was assayed in the presence of KpSSB [60]. Tag-free KpSSB [61] was also used for this cross-species analysis. As shown in Fig 10, SaPriA ATPase activity was significantly stimulated (twelfold) when acting with either KpSSB or tag-free KpSSB. Chemically synthesized KpSSB-Ct (the last 15 amino acids of the KpSSB C terminus) was also used for this analysis and was found to fail to stimulate SaPriA. To determine the possible role of the flexible region, KpSSBc, the C-terminal domain of KpSSB that comprises the flexible region and SSB-Ct (aa 116–174), was also analyzed. When acting with KpSSBc, a slight stimulation of SaPriA ATPase (less than twofold) was observed. Thus, we conclude that KpSSB and KpSSBc, except KpSSB-Ct, exhibited a cross-species stimulation effect for SaPriA.

S161 in SaSsbA determines the stimulation property of SaPriA

The N-terminal domain of SSB proteins is basically conserved in sequence and structure [1, 2], such as those in SaSsbA and EcSSB (Fig 7). As the stimulation of SaPriA was found by acting

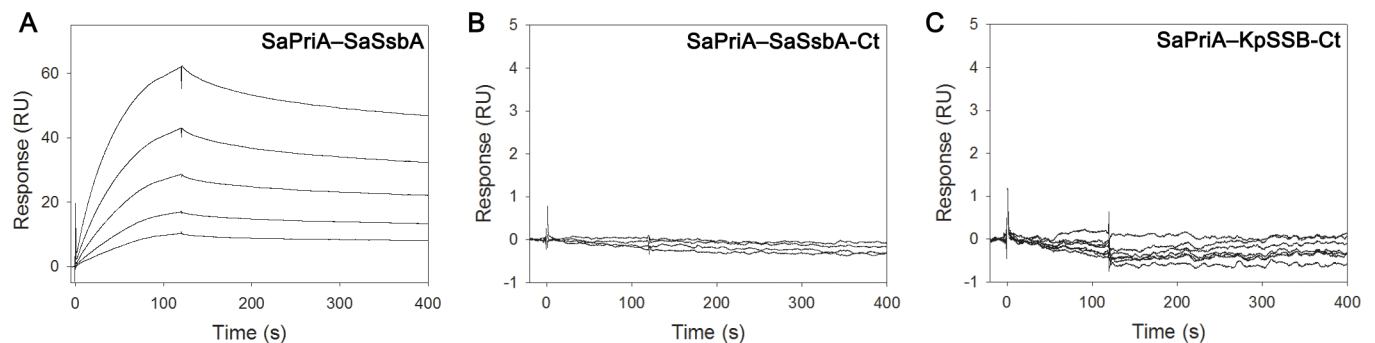


Fig 9. SPR analysis. (A) The SaPriA–SaSsbA interaction. SaPriA was immobilized on Series S sensor chips CM5, and the binding experiments were carried out using a Biacore T200. SaSsbA (1000, 500, 250, 125, and 63 nM) was injected in duplicate over the immobilized protein for 120 s at a flow rate of 30 μ L/min. The estimated K_d value was derived by fitting the association and dissociation signals with a 1:1 (Langmuir) model using the Biacore T200 Evaluation Software. (B) The SaPriA–SaSsbA-Ct interaction analyzed by SPR. (C) The SaPriA–KpSSB-Ct interaction analyzed by SPR.

<https://doi.org/10.1371/journal.pone.0182060.g009>

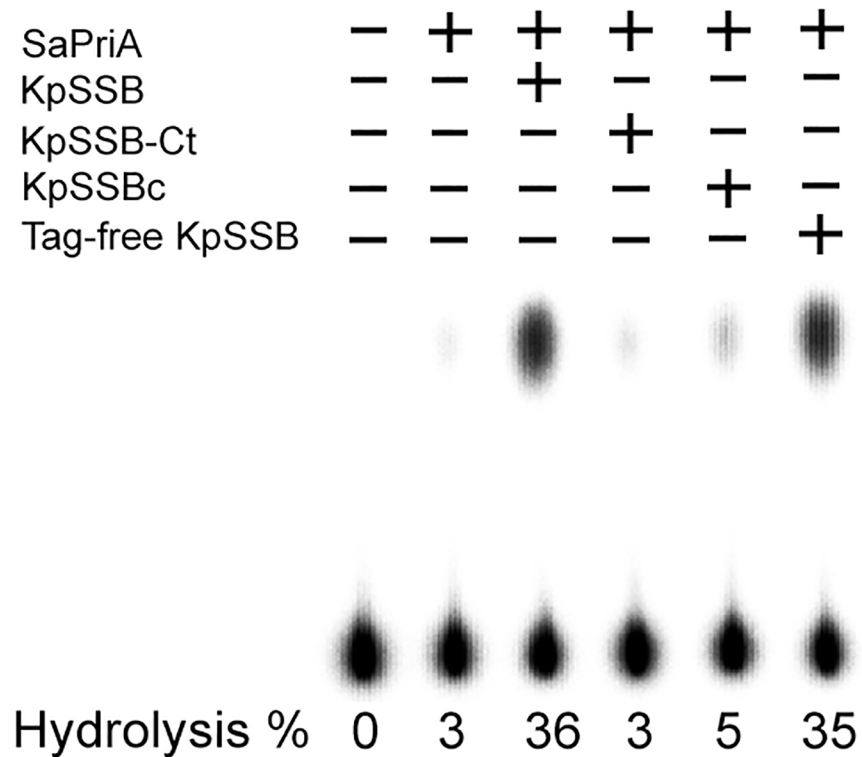


Fig 10. KpSSB, but not KpSSB-Ct, can significantly stimulate the ATPase activity of SaPriA. SaPriA ATPase assay was performed with 0.4 mM [γ - 32 P] ATP, 0.12 μ M of SaPriA, and 0.1 μ M PS4/PS3-dT30 DNA substrate for 1 h. To study the effect, the protein (10 μ M) was individually added into the assay solution. Aliquots (5 μ L) were taken and spotted onto a polyethyleneimine cellulose thin-layer chromatography plate, which was subsequently developed in 0.5 M formic acid and 0.25 M LiCl for 30 m. Reaction products were visualized by autoradiography and quantified with a Phosphorimager.

<https://doi.org/10.1371/journal.pone.0182060.g010>

with KpSSB (Fig 10), but not SaSsbA (Fig 6), we further investigated whether the different SSB-Ct is related to the stimulation switch. We compared the sequence of the C-terminal acidic tails of SSBs and found that the conserved MDFDDDI Δ PF motif in the Gram-negative bacterial SSB, such as Ec, Kp, and St, in which whose motif is DISDDDL Δ PF in SaSsbA, i.e., the amino acid residue F172 in EcSSB and F168 in KpSSB, whose corresponding residue in SaSsbA is S161, not F. To investigate the role of the conserved F residue in SSB proteins (but the residue is S in SaSsbA) in stimulation of PriA activity, SaSsbA S161F mutant was accordingly created with F substitution, and ATPase activity of SaPriA was then assessed (Fig 11). Unlike the wild-type protein, SaPriA ATPase activity was dramatically stimulated when acting with SaSsbA S161F mutant (elevenfold), suggesting that the residue F is important in PriA stimulation. According to sequences, we also constructed the double mutant SaSsbA (S161F/delI160) for analysis with SaPriA; this double mutant, in addition to S161F, whose I160 residue was also deleted. When acting with SaSsbA S161F/delI160 mutant, SaPriA ATPase activity was still stimulated as that with SaSsbA S161F mutant, suggesting a no/minor role of the I160 in PriA stimulation. Overall, based on results from the sequence comparison for the C terminal region in SSB proteins (Fig 11B and S2 Fig) and the ATPase assay, we conclude that S161 in SaSsbA is a switch for SaPriA stimulation. However, it is unclear why the residue F, which is conserved in SSB proteins from the Gram-negative bacteria, is changed to S in SaSsbA.

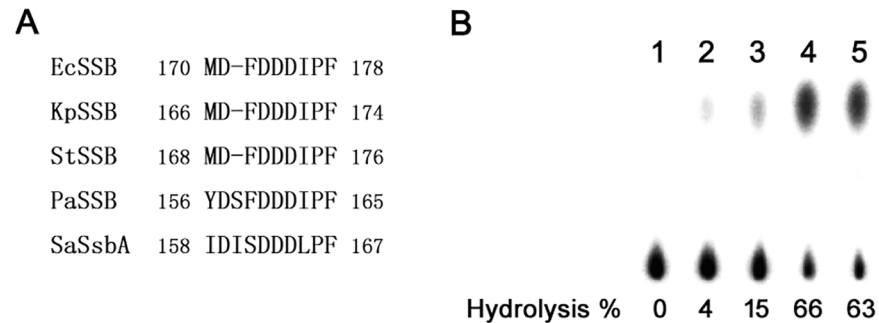


Fig 11. S161 in SaSsbA is a switch for SaPriA stimulation. (A) Multiple amino acid sequence alignment of SSB-Ct from Ec, Kp, St, Pa, and Sa. FDDDIPF in the C-terminal domain of SSB is usually conserved, but is not for SaSsbA. (B) SaPriA ATPase assay was performed with 0.4 mM [γ - 32 P] ATP, 0.12 μ M of SaPriA, and 0.1 μ M PS4/PS3-dT30 DNA substrate for 1 h. To study the effect, the mutant protein was individually added into the assay solution. Aliquots (5 μ L) were taken and spotted onto a polyethyleneimine cellulose thin-layer chromatography plate, which was subsequently developed in 0.5 M formic acid and 0.25 M LiCl for 30 m. Reaction products were visualized by autoradiography and quantified with a Phosphorimager. Reaction was carried out without SaPriA (lane 1) or with SaPriA alone (lane 2) as controls. SaPriA acted with 5 μ M SaSsbA plus 5 μ M SaSsbA S161F mutant (lane 3), 10 μ M SaSsbA S161F (lane 4), and 10 μ M SaSsbA S161F/dell160 double mutant (lane 5) as shown, respectively.

<https://doi.org/10.1371/journal.pone.0182060.g011>

Discussion

It is believed that all cells present now evolved from a common ancestor, implying that the basic principles learned from experiments performed with one type of cell should be generally applicable to other cells. Given the comparative simplicity, *E. coli* has long been the favored organism for studying many fundamental aspects of biochemistry and molecular biology. However, because of many obvious differences in the mechanisms of action of DNA replication restart primosome found between *E. coli* and Gram-positive bacteria [55], the process by which PriA can cooperate with different loading factors to reactivate same stalled forks still need to be elucidated [43, 75]. Gene map analysis shows that unlike *E. coli* *ssb* gene located adjacent to *uvrA* gene, *S. aureus* *ssb* gene (SaSsbA) is flanked by the *rpsF* and *rpsR* genes, coding for the ribosomal proteins S6 and S18, respectively (Fig 1). In this study, we characterized *S. aureus* main SSB and found that it cannot stimulate PriA (Fig 6), unlike *E. coli* [47]. In addition, we also found that the 15 C-terminal amino acids of *E. coli* SSB, known to bind EcPriA, did not bind to SaPriA demonstrated using SPR (Fig 9); that is, in the results of this present study are not in agreement with those for *E. coli*. Whether these significant disparities are due to inherent differences among the species, the use of different assay methods, or the effect of different investigators, remains unknown. However, we also noted that these seemingly contradictory data may reconcile. Our structure-sequence comparison (Figs 7 and 8) and mutational analysis (Fig 11) further indicates that the PriA SSB-Ct binding site (Trp82, Tyr86, Lys370, Arg697, and Gln701), revealed by a 4.1 Å resolution crystal structure [44], is not applicable to SaPriA (Fig 8). Based on these results, we conclude that SaSsbA may bind SaPriA in a different manner compared with that of EcSSB-EcPriA. Whether SaSsbA cannot stimulate SaPriA activity because of this different binding mechanism still remains to be exploited.

The SSB-Ct involved in protein-binding during DNA metabolism is known as the SSB interactome [2]. Studies both in vivo and in vitro using the C-terminal deletion mutants of SSB have found that the last eight residues are important for binding to the target protein, such as RecG and PriA [4, 47, 76–78]. Recently, however, detailed analyses indicate that PXXX motifs in the intrinsically disordered linker (IDL) of SSB are directly responsible for mediating the protein–protein interactions; removal of the last eight residues of SSB with negative effect

on partner protein binding may not be a correct indication of protein–protein interaction site [4, 79, 80]. In this study, both SaSsbA-Ct and KpSSB-Ct peptides did not bind to SaSsbA (Fig 9); thus, we also try to find whether the PXXP motifs are present in SaSsbA. However, unlike EcSSB [4], KpSSB [60], StSSB [81] and PaSSB [82] contain many Pro residues in their C-terminal domains [61], SaSsbA contains very few Pro residues (Fig 3). In addition, their positions in SaSsbA are not able to match the PXXP motif [4]. Whether the Gram-positive and Gram-negative SSB use a general mechanism to bind their partner proteins during DNA metabolism is still unclear.

Almost non-hexameric helicases have poor dsDNA unwinding activities when acting alone in vitro [72]. Recently, the first case for the Gram-positive bacterial PriA activity stimulation has been reported: SaDnaD can obviously enhance the ATPase activity of SaPriA [58]. Like EcSSB, SaSsbA, and EcPriB, SaDnaD can bind ssDNA and PriA [58, 83]. Given that SaSsbA and SaDnaD are both ssDNA- and SaPriA-binding proteins, and both function in early steps of the Gram-positive primosome assembly [75, 84], more studies are still needed to determine whether or not SaSsbA is a competitor or an enhancer for SaDnaD binding to PriA, and PriA bound forked DNA.

Supporting information

S1 Fig. Multiple amino acid sequence alignment of PriA proteins. Sequence alignment of SaPriA, KpPriA, and EcPriA was generated by CLUSTALW2. The KpPriA SSB-Ct binding sites (Trp82, Tyr86, Lys370, Arg697, and Gln701) are colored in red.

(TIF)

S2 Fig. Multiple amino acid sequence alignment of SSB-Ct from some Gram-positive bacteria. Including *Bacillus subtilis*, IDISDDDLPF in the C-terminal domain of SSB from the Gram-positive bacteria is usually conserved.

(TIF)

Acknowledgments

We thank the experimental facility and the technical services provided by the Synchrotron Radiation Protein Crystallography Facility of the National Core Facility Program for Biotechnology, Ministry of Science and Technology and the National Synchrotron Radiation Research Center, a national user facility supported by the Ministry of Science and Technology, Taiwan, ROC.

Author Contributions

Conceptualization: Yen-Hua Huang, Cheng-Yang Huang.

Data curation: Yen-Hua Huang, Cheng-Yang Huang.

Formal analysis: Yen-Hua Huang, Cheng-Yang Huang.

Funding acquisition: Cheng-Yang Huang.

Investigation: Yen-Hua Huang, Cheng-Yang Huang.

Methodology: Yen-Hua Huang, Hong-Hsiang Guan, Cheng-Yang Huang.

Project administration: Cheng-Yang Huang.

Resources: Cheng-Yang Huang.

Software: Yen-Hua Huang, Cheng-Yang Huang.

Supervision: Cheng-Yang Huang.

Validation: Cheng-Yang Huang.

Visualization: Cheng-Yang Huang.

Writing – original draft: Cheng-Yang Huang.

Writing – review & editing: Chun-Jung Chen, Cheng-Yang Huang.

References

1. Richard DJ, Bolderson E, Khanna KK (2009) Multiple human single-stranded DNA binding proteins function in genome maintenance: structural, biochemical and functional analysis. *Crit. Rev. Biochem. Mol. Biol.* 44: 98–116. <https://doi.org/10.1080/10409230902849180> PMID: 19367476
2. Shereda RD, Kozlov AG, Lohman TM, Cox MM, Keck JL (2008) SSB as an organizer/mobilizer of genome maintenance complexes. *Crit. Rev. Biochem. Mol. Biol.* 43: 289–318. <https://doi.org/10.1080/10409230802341296> PMID: 18937104
3. Meyer RR, Laine PS (1990) The single-stranded DNA-binding protein of *Escherichia coli*. *Microbiol. Rev.* 54: 342–380. PMID: 2087220
4. Bianco PR (2016) The tale of SSB. *Prog. Biophys. Mol. Biol.* <https://doi.org/10.1016/j.pbiomolbio.2016.11.001> PMID: 27838363
5. Costes A, Lecointe F, McGovern S, Quevillon-Cheruel S, Polard P (2010) The C-terminal domain of the bacterial SSB protein acts as a DNA maintenance hub at active chromosome replication forks. *PLoS Genet.* 6: e1001238. <https://doi.org/10.1371/journal.pgen.1001238> PMID: 21170359
6. Yang C, Curth U, Urbanke C, Kang C (1997) Crystal structure of human mitochondrial single-stranded DNA binding protein at 2.4 Å resolution. *Nat. Struct. Biol.* 4: 153–157. PMID: 9033597
7. Webster G, Genschel J, Curth U, Urbanke C, Kang C, Hilgenfeld R (1997) A common core for binding single-stranded DNA: structural comparison of the single-stranded DNA-binding proteins (SSB) from *E. coli* and human mitochondria. *FEBS Lett.* 411: 313–316. PMID: 9271227
8. Flynn RL, Zou L (2010) Oligonucleotide/oligosaccharide-binding fold proteins: a growing family of genome guardians. *Crit. Rev. Biochem. Mol. Biol.* 45: 266–275. <https://doi.org/10.3109/10409238.2010.488216> PMID: 20515430
9. Chan KW, Lee YJ, Wang CH, Huang H, Sun YJ (2009) Single-stranded DNA-binding protein complex from *Helicobacter pylori* suggests an ssDNA-binding surface. *J. Mol. Biol.* 388: 508–519. <https://doi.org/10.1016/j.jmb.2009.03.022> PMID: 19285993
10. Theobald DL, Mitton-Fry RM, Wuttke DS (2003) Nucleic acid recognition by OB-fold proteins. *Annu. Rev. Biophys. Biomol. Struct.* 32: 115–133. PMID: 12598368 <https://doi.org/10.1146/annurev.biophys.32.110601.142506>
11. Raghunathan S, Kozlov AG, Lohman TM, Waksman G (2000) Structure of the DNA binding domain of *E. coli* SSB bound to ssDNA. *Nat. Struct. Biol.* 7: 648–652. PMID: 10932248 <https://doi.org/10.1038/77943>
12. Murzin AG (1993) OB(oligonucleotide/oligosaccharide binding)-fold: common structural and functional solution for non-homologous sequences. *EMBO J.* 12: 861–867. PMID: 8458342.
13. George NP, Ngo KV, Chitteni-Pattu S, Norais CA, Battista JR, Cox MM, et al. (2012) Structure and cellular dynamics of *Deinococcus radiodurans* single-stranded DNA (ssDNA)-binding protein (SSB)-DNA complexes. *J. Biol. Chem.* 287: 22123–22132. <https://doi.org/10.1074/jbc.M112.367573> PMID: 22570477
14. Filipkowski P, Kur J (2007) Identification and properties of the *Deinococcus grandis* and *Deinococcus proteolyticus* single-stranded DNA binding proteins (SSB). *Acta Biochim. Pol.* 54: 79–87. PMID: 17325748
15. Filipkowski P, Duraj-Thatte A, Kur J (2007) Identification, cloning, expression, and characterization of a highly thermostable single-stranded-DNA-binding protein (SSB) from *Deinococcus murrayi*. *Protein Expr. Purif.* 53: 201–208. PMID: 17175167 <https://doi.org/10.1016/j.pep.2006.11.006>
16. Filipkowski P, Koziatek M, Kur J (2006) A highly thermostable, homodimeric single-stranded DNA-binding protein from *Deinococcus radiopugnans*. *Extremophiles* 10: 607–614. <https://doi.org/10.1007/s00792-006-0011-8> PMID: 16896528

17. Filipkowski P, Duraj-Thatte A, Kur J (2006) Novel thermostable single-stranded DNA-binding protein (SSB) from *Deinococcus geothermalis*. Arch. Microbiol. 186: 129–137. <https://doi.org/10.1007/s00203-006-0128-2> PMID: 16802171
18. Witte G, Urbanke C, Curth U (2005) Single-stranded DNA-binding protein of *Deinococcus radiodurans*: a biophysical characterization. Nucleic Acids Res. 33: 1662–1670. PMID: 15781492 <https://doi.org/10.1093/nar/gki310>
19. Bernstein DA, Eggington JM, Killoran MP, Mistic AM, Cox MM, Keck JL (2004) Crystal structure of the *Deinococcus radiodurans* single-stranded DNA-binding protein suggests a mechanism for coping with DNA damage. Proc. Natl. Acad. Sci. U. S. A. 101: 8575–8580. <https://doi.org/10.1073/pnas.0401331101> PMID: 15159541
20. Dabrowski S, Olszewski M, Piatek R, Brillowska-Dabrowska A, Konopa G, Kur J (2002) Identification and characterization of single-stranded-DNA-binding proteins from *Thermus thermophilus* and *Thermus aquaticus*—new arrangement of binding domains. Microbiology. 148: 3307–3315. PMID: 12368464 <https://doi.org/10.1099/00221287-148-10-3307>
21. Gamsjaeger R, Kariawasam R, Touma C, Kwan AH, White MF, Cubeddu L. (2014) Backbone and side-chain ¹H, ¹³C and ¹⁵N resonance assignments of the OB domain of the single stranded DNA binding protein from *Sulfolobus solfataricus* and chemical shift mapping of the DNA-binding interface. Biomol. NMR Assign. 8: 243–246. <https://doi.org/10.1007/s12104-013-9492-4> PMID: 23749431
22. Rolfsmeier ML, Haseltine CA (2010) The single-stranded DNA binding protein of *Sulfolobus solfataricus* acts in the presynaptic step of homologous recombination. J. Mol. Biol. 397: 31–45. <https://doi.org/10.1016/j.jmb.2010.01.004> PMID: 20080104
23. Kerr ID, Wadsworth RI, Cubeddu L, Blankenfeldt W, Naismith JH, White MF (2003) Insights into ssDNA recognition by the OB fold from a structural and thermodynamic study of *Sulfolobus* SSB protein. EMBO J. 22: 2561–2570. PMID: 12773373 <https://doi.org/10.1093/emboj/cdg272>
24. Haseltine CA, Kowalczykowski SC (2002) A distinctive single-strand DNA-binding protein from the Archaeon *Sulfolobus solfataricus*. Mol. Microbiol. 43: 1505–1515. PMID: 11971263
25. Wadsworth RI, White MF (2001) Identification and properties of the crenarchaeal single-stranded DNA binding protein from *Sulfolobus solfataricus*. Nucleic Acids Res. 29: 914–920. PMID: 11160923
26. Ghalei H, Moeller HV, Eppers D, Sohmen D, Wilson DN, Loll B, et al. (2014) Entrapment of DNA in an intersubunit tunnel system of a single-stranded DNA-binding protein. Nucleic Acids Res. 42: 6698–6708. <https://doi.org/10.1093/nar/gku259> PMID: 24744237
27. Paytubi S, McMahon SA, Graham S, Liu H, Botting CH, Makarova KS, et al. (2011) Displacement of the canonical single-stranded DNA-binding protein in the *Thermoproteales*. Proc. Natl. Acad. Sci. U. S. A. 109: E398–E405. <https://doi.org/10.1073/pnas.1113277108> PMID: 22106294
28. Dickey TH, Altschuler SE, Wuttke DS (2013) Single-stranded DNA-binding proteins: multiple domains for multiple functions. Structure 21: 1074–1084. <https://doi.org/10.1016/j.str.2013.05.013> PMID: 23823326
29. Olszewski M, Grot A, Wojciechowski M, Nowak M, Mickiewicz M, Kur J (2010) Characterization of exceptionally thermostable single-stranded DNA-binding proteins from *Thermotoga maritima* and *Thermotoga neapolitana*. BMC Microbiol. 10:260. <https://doi.org/10.1186/1471-2180-10-260> PMID: 20950419
30. Witte G, Urbanke C, Curth U (2003) DNA polymerase III chi subunit ties single-stranded DNA binding protein to the bacterial replication machinery. Nucleic Acids Res. 31: 4434–4440. PMID: 12888503
31. Curth U, Genschel J, Urbanke C, Greipel J (1996) In vitro and in vivo function of the C-terminus of *Escherichia coli* single-stranded DNA binding protein. Nucleic Acids Res. 24: 2706–2711. PMID: 8759000
32. Shishmarev D, Wang Y, Mason CE, Su XC, Oakley AJ, Graham B, et al. (2014) Intramolecular binding mode of the C-terminus of *Escherichia coli* single-stranded DNA binding protein determined by nuclear magnetic resonance spectroscopy. Nucleic Acids Res. 42: 2750–2757. <https://doi.org/10.1093/nar/gkt1238> PMID: 24288378
33. Kozlov AG, Cox MM, Lohman TM (2010) Regulation of single-stranded DNA binding by the C termini of *Escherichia coli* single-stranded DNA-binding (SSB) protein. J. Biol. Chem. 285: 17246–17252. <https://doi.org/10.1074/jbc.M110.118273> PMID: 20360609
34. Lohman TM, Ferrari ME (1994) *Escherichia coli* single-stranded DNA-binding protein: multiple DNA-binding modes and cooperativities. Annu. Rev. Biochem. 63: 527–570. <https://doi.org/10.1146/annurev.bi.63.070194.002523> PMID: 7979247
35. Zhou R, Kozlov AG, Roy R, Zhang J, Korolev S, Lohman TM, et al. (2011) SSB functions as a sliding platform that migrates on DNA via reptation. Cell 146: 222–232. <https://doi.org/10.1016/j.cell.2011.06.036> PMID: 21784244

36. Roy R, Kozlov AG, Lohman TM, Ha T (2009) SSB protein diffusion on single-stranded DNA stimulates RecA filament formation. *Nature* 461: 1092–1097. <https://doi.org/10.1038/nature08442> PMID: 19820696
37. Roy R, Kozlov AG, Lohman TM, Ha T (2007) Dynamic structural rearrangements between DNA binding modes of *E. coli* SSB protein. *J. Mol. Biol.* 369: 1244–1257. PMID: 17490681 <https://doi.org/10.1016/j.jmb.2007.03.079>
38. Sandler SJ, Mariani KJ (2000) Role of PriA in replication fork reactivation in *Escherichia coli*. *J. Bacteriol.* 182: 9–13. PMID: 10613856
39. Mariani KJ (2000) PriA-directed replication fork restart in *Escherichia coli*. *Trends Biochem. Sci.* 25: 185–189. PMID: 10754552
40. Ng JY, Mariani KJ (1996) The ordered assembly of the phiX174-type primosome. I. Isolation and identification of intermediate protein-DNA complexes. *J. Biol. Chem.* 271: 15642–15648. PMID: 8663104
41. Allen GC Jr., Dixon NE, Kornberg A (1993) Strand switching of a replicative DNA helicase promoted by the *E. coli* primosome. *Cell* 74: 713–722. PMID: 8395352
42. Ouzounis CA, Blencowe BJ (1991) Bacterial DNA replication initiation factor priA is related to proteins belonging to the 'DEAD-box' family. *Nucleic Acids Res.* 19: 6953. PMID: 1662369
43. Huang YH, Huang CY (2014) Structural insight into the DNA-binding mode of the primosomal proteins PriA, PriB, and DnaT. *Biomed Res. Int.* 2014: 195162. <https://doi.org/10.1155/2014/195162> PMID: 25136561
44. Bhattacharyya B, George NP, Thurmes TM, Zhou R, Jani N, Wessel SR, et al. (2014) Structural mechanisms of PriA-mediated DNA replication restart. *Proc. Natl. Acad. Sci. U. S. A.* 111: 1373–1378. <https://doi.org/10.1073/pnas.1318001111> PMID: 24379377
45. Masai H, Tanaka T, Kohda D (2010) Stalled replication forks: making ends meet for recognition and stabilization. *Bioessays* 32: 687–697. <https://doi.org/10.1002/bies.200900196> PMID: 20658707
46. Cadman CJ, Lopper M, Moon PB, Keck JL, McGlynn P (2005) PriB stimulates PriA helicase via an interaction with single-stranded DNA. *J. Biol. Chem.* 280: 39693–39700. <https://doi.org/10.1074/jbc.M508521200> PMID: 16188886
47. Cadman CJ, McGlynn P (2004) PriA helicase and SSB interact physically and functionally. *Nucleic Acids Res.* 32: 6378–6387. <https://doi.org/10.1093/nar/gkh980> PMID: 15576682
48. Wessel SR, Cornilescu CC, Cornilescu G, Metz A, Leroux M, Hu K, et al. (2016) Structure and function of the PriC DNA replication restart protein. *J. Biol. Chem.* 291: 18384–18396. <https://doi.org/10.1074/jbc.M116.738781> PMID: 27382050
49. Huang CC, Huang CY (2016) DnaT is a PriC-binding protein. *Biochem. Biophys. Res. Commun.* 477: 988–992. <https://doi.org/10.1016/j.bbrc.2016.07.016> PMID: 27387236
50. Liu Z, Chen P, Wang X, Cai G, Niu L, Teng M, et al. (2014) Crystal structure of DnaT84–153-dT10 ssDNA complex reveals a novel single-stranded DNA binding mode. *Nucleic Acids Res.* 42: 9470–9483. <https://doi.org/10.1093/nar/gku633> PMID: 25053836
51. Wessel SR, Marceau AH, Massoni SC, Zhou R, Ha T, Sandler SJ, et al. (2013) PriC-mediated DNA replication restart requires PriC complex formation with the single-stranded DNA-binding protein. *J. Biol. Chem.* 288: 17569–17578. <https://doi.org/10.1074/jbc.M113.478156> PMID: 23629733
52. Huang YH, Lin MJ, Huang CY (2013) DnaT is a single-stranded DNA binding protein. *Genes Cells* 18: 1007–1019. <https://doi.org/10.1111/gtc.12095> PMID: 24118681
53. Huang YH, Huang CY (2013) The N-terminal domain of DnaT, a primosomal DNA replication protein, is crucial for PriB binding and self-trimerization. *Biochem. Biophys. Res. Commun.* 442: 147–152. <https://doi.org/10.1016/j.bbrc.2013.11.069> PMID: 24280305
54. Michel B, Sandler SJ (2017) Replication restart in bacteria. *J. Bacteriol.* <https://doi.org/10.1128/jb.00102-17> PMID: 28320884
55. Briggs GS, Smits WK, Soutanas P (2012) Chromosomal replication initiation machinery of low-G+C-content Firmicutes. *J. Bacteriol.* 194: 5162–5170. <https://doi.org/10.1128/JB.00865-12> PMID: 22797751
56. Bruand C, Ehrlich SD, Janniere L (1995) Primosome assembly site in *Bacillus subtilis*. *EMBO J.* 14: 2642–2650. PMID: 7781616
57. Bruand C, Farache M, McGovern S, Ehrlich SD, Polard P (2001) DnaB, DnaD and DnaI proteins are components of the *Bacillus subtilis* replication restart primosome. *Mol. Microbiol.* 42: 245–255. PMID: 11679082
58. Huang YH, Lien Y, Huang CC, Huang CY (2016) Characterization of *Staphylococcus aureus* primosomal DnaD protein: highly conserved C-terminal region is crucial for ssDNA and PriA helicase binding

- but not for DnaA protein-binding and self-tetramerization. *PLoS One*. 11: e0157593. <https://doi.org/10.1371/journal.pone.0157593> PMID: 27304067
59. Huang YH, Huang CC, Chen CC, Yang KJ, Huang CY (2015) Inhibition of *Staphylococcus aureus* PriA helicase by flavonol kaempferol. *Protein J*. 34: 169–172. <https://doi.org/10.1007/s10930-015-9609-y> PMID: 25894858
 60. Huang YH, Huang CY (2012) Characterization of a single-stranded DNA-binding protein from *Klebsiella pneumoniae*: mutation at either Arg73 or Ser76 causes a less cooperative complex on DNA. *Genes cells* 17: 146–157. <https://doi.org/10.1111/j.1365-2443.2011.01577.x> PMID: 22244199
 61. Huang YH, Huang CY (2014) C-terminal domain swapping of SSB changes the size of the ssDNA binding site. *Biomed Res. Int*. 2014: 573936. <https://doi.org/10.1155/2014/573936> PMID: 25162017
 62. Bradford MM (1976) A rapid and sensitive method for the quantitation of microgram quantities of protein utilizing the principle of protein-dye binding. *Anal. Biochem*. 72: 248–254 PMID: 942051
 63. Huang CY, Hsu CH, Sun YJ, Wu HN, Hsiao CD (2006) Complexed crystal structure of replication restart primosome protein PriB reveals a novel single-stranded DNA-binding mode. *Nucleic Acids Res*. 34: 3878–3886. <https://doi.org/10.1093/nar/gkl536> PMID: 16899446
 64. Huang CY (2012) Determination of the binding site-size of the protein-DNA complex by use of the electrophoretic mobility shift assay. In: *Stoichiometry and Research—The Importance of Quantity in Biomedicine* (ed. Innocenti A) pp.235-242. Rijeka, Croatia: InTech Press.
 65. Lo YH, Tsai KL, Sun YJ, Chen WT, Huang CY, Hsiao CD (2009) The crystal structure of a replicative hexameric helicase DnaC and its complex with single-stranded DNA. *Nucleic Acids Res*. 37: 804–814. <https://doi.org/10.1093/nar/gkn999> PMID: 19074952
 66. Otwinowski Z, Minor W (1997) Processing of X-ray Diffraction Data Collected in Oscillation Mode. *Methods Enzymol*. 276: 307–326.
 67. Navaza J (1994) AMoRe: an automated package for molecular replacement. *Acta Crystallogr*. 50: 157–163.
 68. McRee DE (1999) XtalView/Xfit—A versatile program for manipulating atomic coordinates and electron density. *J. Struct. Biol*. 125: 156–165. <https://doi.org/10.1006/jsbi.1999.4094> PMID: 10222271
 69. Brunger AT, Adams PD, Clore GM, DeLano WL, Gros P, Grosse-Kunstleve RW, et al. (1998) Crystallography & NMR system: A new software suite for macromolecular structure determination. *Acta Crystallogr. D Biol. Crystallogr*. 54: 905–921. PMID: 9757107
 70. Landau M, Mayrose I, Rosenberg Y, Glaser F, Martz E, Pupko T, et al. (2005) ConSurf 2005: the projection of evolutionary conservation scores of residues on protein structures. *Nucleic Acids Res*. 33: W299–W302. <https://doi.org/10.1093/nar/gki370> PMID: 15980475
 71. Lindner C, Nijland R, van Hartskamp M, Bron S, Hamoen LW, Kuipers OP. (2004) Differential expression of two paralogous genes of *Bacillus subtilis* encoding single-stranded DNA binding protein. *J. Bacteriol*. 186: 1097–1105. PMID: 14762004 <https://doi.org/10.1128/JB.186.4.1097-1105.2004>
 72. Lohman TM, Tomko EJ, Wu CG (2008) Non-hexameric DNA helicases and translocases: mechanisms and regulation. *Nat. Rev. Mol. Cell. Biol*. 9: 391–401. <https://doi.org/10.1038/nrm2394> PMID: 18414490
 73. Kozlov AG, Jezewska MJ, Bujalowski W, Lohman TM (2010) Binding specificity of *Escherichia coli* single-stranded DNA binding protein for the chi subunit of DNA pol III holoenzyme and PriA helicase. *Biochemistry* 49: 3555–3566. <https://doi.org/10.1021/bi100069s> PMID: 20329707
 74. Lecointe F, Serena C, Velten M, Costes A, McGovern S, Meile JC, et al. (2007) Anticipating chromosomal replication fork arrest: SSB targets repair DNA helicases to active forks. *EMBO J*. 26: 4239–4251. <https://doi.org/10.1038/sj.emboj.7601848> PMID: 17853894
 75. Velten M, McGovern S, Marsin S, Ehrlich SD, Noirot P, Polard P (2003) A two-protein strategy for the functional loading of a cellular replicative DNA helicase. *Mol. Cell* 11: 1009–1020. PMID: 12718886
 76. Tan HY, Wilczek LA, Pottinger S, Manos M, Yu C, Nguyenduc T, et al. (2017) The intrinsically disordered linker of *E. coli* SSB is critical for the release from single-stranded DNA. *Protein Sci*. 26: 700–717. <https://doi.org/10.1002/pro.3115> PMID: 28078720
 77. Yu C, Tan HY, Choi M, Stanenas AJ, Byrd AK, K DR, et al. (2016) SSB binds to the RecG and PriA helicases in vivo in the absence of DNA. *Genes Cells* 21: 163–184. <https://doi.org/10.1111/gtc.12334> PMID: 26766785
 78. Buss JA, Kimura Y, Bianco PR (2008) RecG interacts directly with SSB: implications for stalled replication fork regression. *Nucleic Acids Res*. 36: 7029–7042. <https://doi.org/10.1093/nar/gkn795> PMID: 18986999
 79. Bianco PR, Pottinger S, Tan HY, Nguyenduc T, Rex K, Varshney U (2017) The IDL of *E. coli* SSB links ssDNA and protein binding by mediating protein-protein interactions. *Protein Sci*. 26: 227–241. <https://doi.org/10.1002/pro.3072> PMID: 28127816

80. Bianco PR, Lyubchenko YL (2017) SSB and the RecG DNA helicase: an intimate association to rescue a stalled replication fork. *Protein Sci.* 26: 638–649. <https://doi.org/10.1002/pro.3114> PMID: 28078722
81. Huang YH, Lee YL, Huang CY (2011) Characterization of a single-stranded DNA binding protein from *Salmonella enterica* serovar Typhimurium LT2. *Protein J.* 30: 102–108. <https://doi.org/10.1007/s10930-011-9309-1> PMID: 21267641
82. Jan HC, Lee YL, Huang CY (2011) Characterization of a single-stranded DNA-binding protein from *Pseudomonas aeruginosa* PAO1. *Protein J.* 30: 20–26. <https://doi.org/10.1007/s10930-010-9297-6> PMID: 21132356
83. Marston FY, Grainger WH, Smits WK, Hopcroft NH, Green M, Hounslow AM, et al. (2010) When simple sequence comparison fails: the cryptic case of the shared domains of the bacterial replication initiation proteins DnaB and DnaD. *Nucleic Acids Res.* 38: 6930–6942. <https://doi.org/10.1093/nar/gkq465> PMID: 20587500
84. Marsin S, McGovern S, Ehrlich SD, Bruand C, Polard P (2001) Early steps of *Bacillus subtilis* primosome assembly. *J. Biol. Chem.* 276: 45818–45825. <https://doi.org/10.1074/jbc.M101996200> PMID: 11585815.